

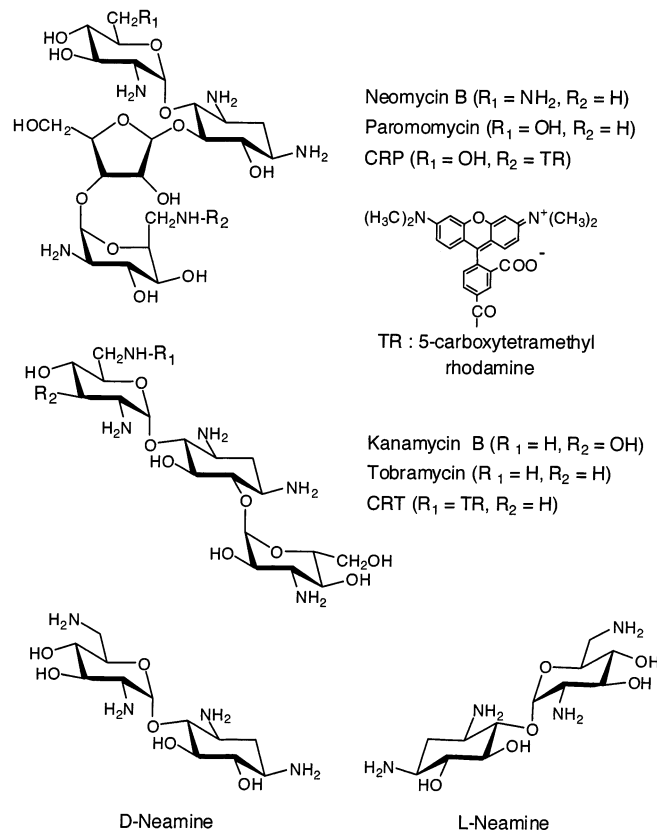
in the μM range are found for the interactions of aminoglycosides and RNA molecules (10–14). RNA molecules that bind to aminoglycosides typically possess nonduplex structural elements (17, 18). Often these RNA molecules contain asymmetric bulges or bubbles, which allow aminoglycoside access to the purine and pyrimidine bases (10–18).

Since aminoglycosides are among the most clinically important group of drugs known to target RNA molecules, it is important to establish the order of selectivity of this class of drugs. To begin with, it is unlikely that a high degree of specificity is involved because of the broadly diverse nature of the structures of aminoglycoside antibiotics thought to share the same decoding region target (1–6). Moreover, as mentioned above, structurally diverse aminoglycosides bind to a broad collection of RNA molecules with similar affinities. These observations are inconsistent with a high degree of specificity in the binding interactions between aminoglycosides and their pharmacological targets. Further probing of the specificity of aminoglycoside–target interactions also addresses this central issue governing drug–RNA interactions in general, and aminoglycoside–RNA interactions in particular. This could potentially lead to the design of novel antagonists, which might avoid some of the difficulties inherent in the use of aminoglycosides; namely, low potency, toxicity, and the ready development of resistance (6). The experiments reported here were designed to address the issue of stereospecificity (mirror image specificity) of aminoglycoside binding to the bacterial rRNA decoding region.

Stereospecificity in ligand binding is clearly central to binding specificity. It is well known that enzymes and protein receptors usually show preferential binding of one enantiomer of a ligand relative to its mirror image. In the present study, the stereospecificity of aminoglycoside binding to ribosomal decoding regions is addressed. Several approaches are reported. First, the stereospecificity of aminoglycoside binding to bacterial decoding region rRNA constructs was determined. The experiments were performed in two ways. First, the binding of naturally occurring D-aminoglycosides to both D- (natural stereochemistry) and L-decoding region constructs was determined. Second, the binding of natural D-neamine and its mirror image, L-neamine, to the D- and L-A-site decoding region construct was investigated. Interestingly, the binding is observed to be only weakly stereospecific in both types of experiments.

While there are clearly elements of specificity in the binding of aminoglycosides to the small RNA constructs, as determined by NMR investigations (e.g., 19, 20), whether these constructs are predictive of aminoglycoside binding and functional effects on intact ribosomes is another question. Therefore, in the second approach reported, the model work on aminoglycoside binding to A-site constructs is extended to intact ribosomes and bacteria. While the binding affinities of D/L-neamines to the RNA constructs and prokaryotic ribosomes are similar, there is a distinct difference in the potencies of these aminoglycosides with respect to interfering with protein synthesis. L-Neamine is approximately 5-fold less potent than its D-enantiomer. This decreased potency carries over to in vivo studies on Gram (–) bacteria. Interestingly though, Gram (–) bacteria resistant to D-neamine are not resistant to L-neamine. This suggests the possibility that aminoglycosides of the L-series may be inherently

Scheme 2: Structures of Neomycin B, Paromomycin, Kanamycin B, Tobramycin, CRP, CRT, and D- and L-Neamine



resistant to enzyme-mediated detoxification events insofar as these processes are strongly stereospecific in nature.

EXPERIMENTAL PROCEDURES

Materials. The structures of aminoglycosides, used in the study, are shown in Scheme 2. Neomycin sulfate, paromomycin sulfate, kanamycin B sulfate, tobramycin sulfate, and streptomycin sulfate were purchased from Sigma Inc. and used without further purification. 5-Carboxytetramethyl-rhodamine-labeled paromomycin (CRP) and tobramycin (CRT) were prepared as previously reported (21). L-Ribonucleoside phosphoramidites and L-ribonucleoside CPG supports were purchased from ChemGenes Inc. Nick Sephadex G-50 columns were purchased from Pharmacia Inc. D-Neamine hydrochloride was synthesized from Neomycin B sulfate as described previously (22). The synthesis of L-neamine hydrochloride starting from 2-deoxystreptamine and L-glucosamine will be described elsewhere.

Methods. Synthesis of L- and D-Oligonucleotides. The oligomers were synthesized on an Expedite oligonucleotide synthesizer using a modified 1 μmol RNA cycle, L(D)-ribonucleoside CPG supports, DMT-L(D)-ribonucleoside phosphoramidites, and a coupling time of 600s. After deblocking with ethanolic ammonium hydroxide and triethylamine trihydrofluoride, we precipitated the oligoribonucleotides with *n*-butanol at -20°C (23) and desalted them on a Nick Sephadex G-50 column. The oligonucleotides were purified by gel-electrophoresis on a 12% polyacrylamide/7M urea denaturing gel. All stock solutions were prepared in nuclease-free water and were diluted with the appropriate

buffers prior to use. The concentrations of RNA oligonucleotides were determined spectrophotometrically, by absorption at 260 nm. The RNA molecules were annealed by heating to 95 °C, followed by cooling to room temperature. For the comparison, D-A-site RNA construct was also purchased from Dharmacon and was deprotected using the buffer provided and according to the company's instructions.

Fluorescence Measurements. 5-Carboxytetramethylrhodamine-labeled paromomycin (CRP) and tobramycin (CRT) concentrations were determined spectroscopically at 550 nm using a molar extinction coefficient of $6.00 \times 10^4 \text{ M}^{-1} \text{ cm}^{-1}$ (21). Fluorescence anisotropy measurements were performed on a Perkin-Elmer LS-50B luminescence spectrometer equipped with a thermostat accurate to ± 0.1 °C as indicated previously (21). The tracer solution was excited at 550 nm and monitored at 580 nm. The integration time was 5 s. For every point, 6–10 measurements were taken, and their average values were used for calculation. Measurements were carried out in a buffer solution containing 150 mM NaCl, 5 mM KCl, 1 mM CaCl_2 , 1 mM MgCl_2 , and 20 mM HEPES (pH 7.5). Prior to measurements, RNA constructs were renatured by incubating in binding buffer [150 mM NaCl, 5 mM KCl, 1 mM CaCl_2 , 1 mM MgCl_2 , and 20 mM HEPES (pH 7.5)] for 3 min at 90 °C, followed by cooling to 25 °C.

Determination of Binding Dissociation Constants. Equation 1 was used for the determination of the dissociation constant (K_d) for the interactions between RNA or ribosome and CRP (12, 21)

$$A = A_0 + \Delta A \{ [\text{RNA}]_0 + [\text{CRP}]_0 + K_d - \{ ([\text{RNA}]_0 + [\text{CRP}]_0 + K_d)^2 - 4[\text{RNA}]_0[\text{CRP}]_0 \}^{1/2} \} / 2 \quad (1)$$

where A and A_0 are the fluorescence anisotropy of CRP in the presence and absence of RNA, respectively, and ΔA is the fluorescence anisotropy of CRP in the presence of an extrapolated infinite concentration of RNA minus the fluorescence anisotropy in the absence of RNA. $[\text{RNA}]_0$ and $[\text{CRP}]_0$ are the initial concentrations of RNA and CRP, respectively.

Equation 2 is used for the calculation of the K_D values in the competition binding assay

$$[\text{aminoglycoside}]_0 = \frac{[K_D(A_\infty - A)/K_d(A - A_0) + 1][[\text{RNA}]_0 - K_d(A - A_0)]}{(A_\infty - A) - [\text{CRP}]_0(A - A_0)/(A_\infty - A)} \quad (2)$$

where K_D is the dissociation constant between the RNA and the aminoglycosides. $[\text{aminoglycoside}]_0$ is the initial concentration of the aminoglycosides. Both K_d and K_D were determined by nonlinear curve fitting using the equations described above and are presented as mean values of three independent measurements.

Preparation of Ribosomes. *E. coli* 70S Ribosomes. The purification of *E. coli* (MRE600) 70S ribosomes was carried out according to the published procedures (24). *Escherichia coli* MRE600 was grown for 12 h in 6 L of LB medium (10 g of trypton, 5 g of yeast extract, 5 g of NaCl per 1 L, pH 7.0) at 37 °C. Crude ribosomes were precipitated from clarified supernatant by 4 h centrifugation at 25 000 rpm in Beckman SW 28 rotor at 4 °C. The ribosomal pellets were

collected in 5 mL of buffer BR1, containing 10 mM HEPES, pH 7.5, 500 mM ammonium acetate, 100 mM magnesium chloride, and 2.5 mM DTT. The ribosomal suspension was centrifuged for 20 min at 15 000 rpm to clarify. The clarified sample was loaded over two layers of 20% and 40% sucrose in buffer BR1 and centrifuged for 18 h at 19 000 rpm in Beckman SW28 rotor at 4 °C. The supernatant was carefully discarded, and the purified ribosome pellet was resuspended in buffer BR2 containing 20 mM HEPES, pH 7.5, 50 mM ammonium chloride, 12 mM magnesium chloride, and 1 mM DTT. The concentrations of ribosomes were determined by absorbance at 260 nm, assuming 23 pmol/OD₂₆₀, and the ribosomal suspension was frozen in liquid nitrogen and stored at -80 °C.

Yeast 80S Ribosomes. The purification of yeast 80S ribosomes from *Saccharomyces cerevisiae* strain YSB 758 was carried out according to the published procedure (25). *S. cerevisiae* YSB 758 were grown for 12 h at 30 °C in 2 L of YPD medium, containing 20 g of bactopectone, 20 g of glucose, 10 g of yeast extract, and 0.15 g of tryptophan per 1 L, pH 7.0. The cells were lysed by 10 cycles of 1 min vigorous shaking with glass beads using a vortex, followed by cooling on ice. Clarified cell extract (about 9 mL total, used in 6 portions in 1.5 mL aliquots) was carefully loaded on top of 2 mL of a "cushion", composed of 10% sucrose and 5% ammonium sulfate dissolved in buffer YR1 (20 mM HEPES, pH 7.4, 16 mM magnesium chloride, 100 mM potassium chloride, 5 mM DTT, and 0.5 mM EDTA). The ribosomes were collected by centrifugation in Beckman TL100.3 rotor at 75 000 rpm for 3 h. The supernatants were carefully discarded and ribosomes were collected in buffer YR1. The ribosome suspension was clarified by centrifugation at 14 000 rpm in an Eppendorf centrifuge, and pellets were discarded. Ribosome concentrations were determined by absorbance at 260 nm, assuming 18 pmol of 80S ribosome particles per 1 OD₂₆₀. Ribosomes were frozen in liquid nitrogen and stored at -80 °C.

In Vitro Translation. *In vitro* translation was performed by using PROTEINscript-PRO (Ambion) kit. This kit is designed for coupled *in vitro* transcription and translation using a highly active *E. coli* S30 extract, containing 70S ribosomes. Reaction mixtures contained appropriate concentrations of antibiotic (neomycin B, D- and L-neamine). The protein was translated from CAT mRNA, transcribed from control DNA template containing CAT gene under control of the T7 promoter. The product, ~25 kDa chloramphenicol acetyl transferase, was labeled during translation with 1 μCi ³⁵S methionine (New England Nuclear) per reaction (no cold methionine was added).

Following the translation, the samples were analyzed by electrophoresis on 4–20% SDS minigels (Invitrogen) for 1.5 h at 120 V. Gels were fixed with 40% methanol/10% acetic acid and exposed to Molecular Dynamics phosphorimager plates, which were read on a Personal FX phosphorimager (Bio-Rad) and quantitated using QuantityOne software.

Antibiotic Activity Disk Assays. *E. coli* (ATCC 25922) and *Pseudomonas aeruginosa* (ATCC 27853) (BD Bioscience) were inoculated in 3 mL of medium 2 (BD Bioscience), containing 6 g of peptone, 3 g of yeast extract and 1.5 g of beef extract per 1 L, pH 6.6, and were grown in a shaker for 6 h at 37 °C until OD₅₆₀ = 0.6–0.8 was reached. Alternatively Mueller-Hinton broth (BD Bioscience), containing 2

g of beef extract, 17.5 g of casamino acids, 1.5 g of starch per 1 L, pH 7.3, was used. Growing bacteria in both media produced similar results. Kanamycin/neomycin-resistant *E. coli* was prepared by transformation (electroporation) of wild-type (WT) *E. coli* (ATCC 25922) with pMM plasmid, bearing the aminoglycoside phosphotransferase II (APH(3')-IIa) gene (NPT II, EC 2.7.1.95) (26). Kanamycin/neomycin-resistant *E. coli* was propagated in the same medium 2, supplemented with 30 $\mu\text{g/mL}$ kanamycin.

For the antibiotic disk assay, 50 μL of each bacterial inoculum was mixed with 10 mL of melted agar (1.5% medium 2 agar, BD Bioscience) at 50–55 $^{\circ}\text{C}$ and poured onto 100 mm Petri dishes. Sterile Whatmann 3 MM 5 mm paper disks were soaked with antibiotic solutions and allowed to dry. The disks were positioned evenly on the surface of bacterial-inoculated solid agar, and the plates were incubated at 37 $^{\circ}\text{C}$ for 1–2 days.

MIC and Bactericide Index Measurements. Minimal inhibitory concentrations (MIC) were measured according to the published method (27). *E. coli* (ATCC 25922) (both wild type and pMM-transformed) and *P. aeruginosa* (ATCC 27853) were grown in medium 2 of Mueller–Hinton broth to an optical density OD_{600} of 0.6–0.8. The inoculi were diluted to $\text{OD}_{600} \sim 0.1$ in medium 2 and 1 mL of the culture was placed in 13 mL test tubes. The desired concentrations of antibiotic were added from stock solutions. The samples were incubated at 37 $^{\circ}\text{C}$ for 3–5 h when the control culture had an OD_{600} of 1.2–1.5. The absorbance at 600 nm of each sample was read, and the MIC was taken as the lowest antibiotic concentration inhibiting bacterial growth by greater than 90%.

The bactericidal activity of each antibiotic was investigated at concentrations of 0.5–4 \times MIC in medium 2. *E. coli* (ATCC 25922) inoculum was added to 0.5 mL medium 2 to $\text{OD}_{600} \sim 0.1$, together with different antibiotic concentrations. The samples were incubated at 37 $^{\circ}\text{C}$ for 3 h, and the bacteria were collected by centrifugation. The bacterial pellets were washed with 0.5 mL of medium 2 and were plated on 1.5% medium 2 agar in 100 mm Petri dishes. The plates were incubated for 1–2 days at 37 $^{\circ}\text{C}$, and the mean log change in viable count was calculated and plotted versus log of drug concentration (28).

RESULTS

Binding of Aminoglycosides to D- and L-RNA Constructs. Initial experiments were aimed at determining whether aminoglycoside binding to an A-site decoding region construct (19, 21) is stereospecific or not. These binding studies were performed on the small rRNA constructs, shown in Scheme 1 (19, 21). The two constructs shown are a bacterial 16S A-site rRNA construct (A-site) (19) and an RNA aptamer (J6f1) selected to bind to the aminoglycoside tobramycin (12, 15, 16). Aminoglycoside binding to J6f1 is of interest because of the high level of binding specificity observed with this aptamer (12, 15, 16), making it a useful control for binding studies on the decoding region constructs. Enantiomeric aminoglycosides are not readily available, so the binding experiments were carried out using chemically synthesized enantiomeric D- (natural) and L-RNA constructs. The two constructs A-site and J6f1 were prepared from D- and L-ribonucleotides. Circular dichroism spectra of the

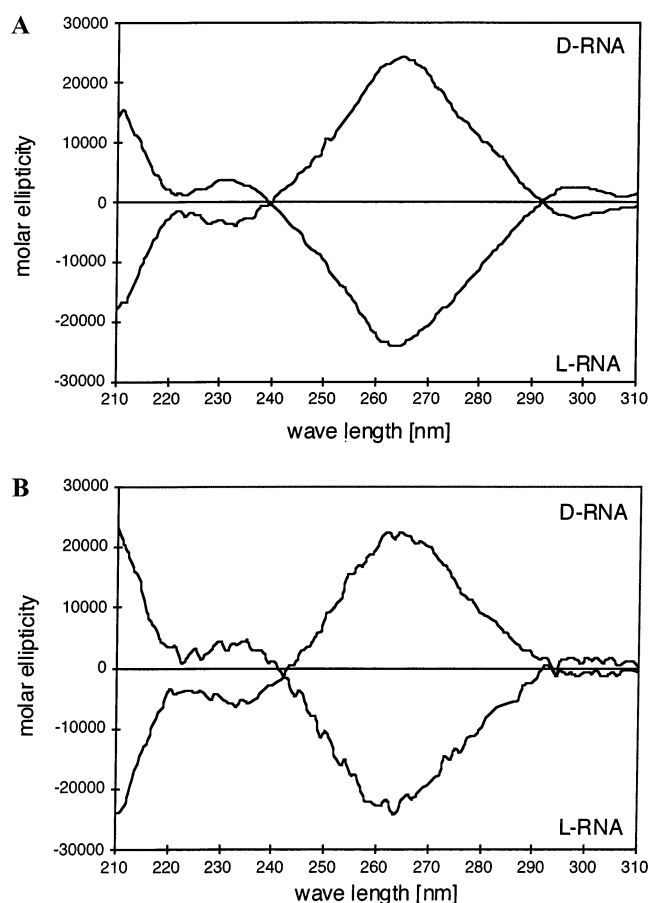


FIGURE 1: (A, B) Circular dichroism (CD) spectra of A-site (A) and J6f1 (B) RNA constructs. The experiments were performed by mixing 50 μL stock solution + 450 μL 100 mM sodium chloride, 10 mM sodium hydrogen phosphate, pH 7.0, at 4 $^{\circ}\text{C}$ on an Aviv 202 spectropolarimeter.

purified synthetic RNA constructs confirm their mirror-image relationships (Figure 1A,B). These D- and L-RNA constructs were tested for aminoglycoside binding using the fluorescence anisotropy method, previously developed in our laboratory (12, 16, 17). In these measurements, the fluorescent aminoglycoside CRP (Scheme 2) was used to monitor binding to the decoding region constructs (A-site), and CRT (Scheme 2) was used to monitor binding to J6f1, as this aptamer was selected to bind tobramycin (12, 16, 17). The binding of CRP to L-A-site and CRT to L-J6f1 is shown in panels A and B, respectively, of Figure 2. To measure the stereospecificity of aminoglycoside binding, we studied the competition of various aminoglycosides with CRP or CRT for binding to the D- and L-RNA constructs. Typical competition experiments using paromomycin binding to the mirror-image decoding region, L-A-site (Scheme 1) and tobramycin to the mirror-image aptamer L-J6f1 (Scheme 1) are shown in Figure 3A,B. Table 1 provides the data for the binding of various aminoglycosides to the enantiomeric decoding region constructs and to the D- and L-J6f1 enantiomers. These data indicate that aminoglycoside binding to the prokaryotic decoding region A-site construct is weakly stereospecific. In contrast, aminoglycoside binding to the aptamer J6f1 is, as expected, strongly stereospecific. The measured affinities for the D-decoding region construct is consistent with results of binding measurements on prokaryotic ribosomes using radioactive tobramycin (29). Binding affinities in the micro-

Table 1: K_d , K_D , NM, of RNA–Aminoglycoside Complexes at 20 °C

aminoglycoside	D-A site construct	L-A site construct	D-J6f1 aptamer	L-J6f1 aptamer
CRP(T) (K_d)	170.0 ± 17.5^a	224.0 ± 22.6^a	190 ± 1.1^b	200 ± 28^b
neomycin B	51.96 ± 1.86	109.1 ± 4.6	5590 ± 139	360 ± 21
paromomycin	1650 ± 350	6380 ± 27	— ^c	4600 ± 370
kanamycin B	1250 ± 70	810 ± 95	22 ± 4.7	3340 ± 250
tobramycin	1400 ± 240	4390 ± 370	5.2 ± 0.42	2180 ± 230
D-neamine	501.7 ± 14.2	995.4 ± 27.8	— ^c	— ^c
L-neamine	1039.5 ± 29.1	426.9 ± 10.7	— ^c	— ^c

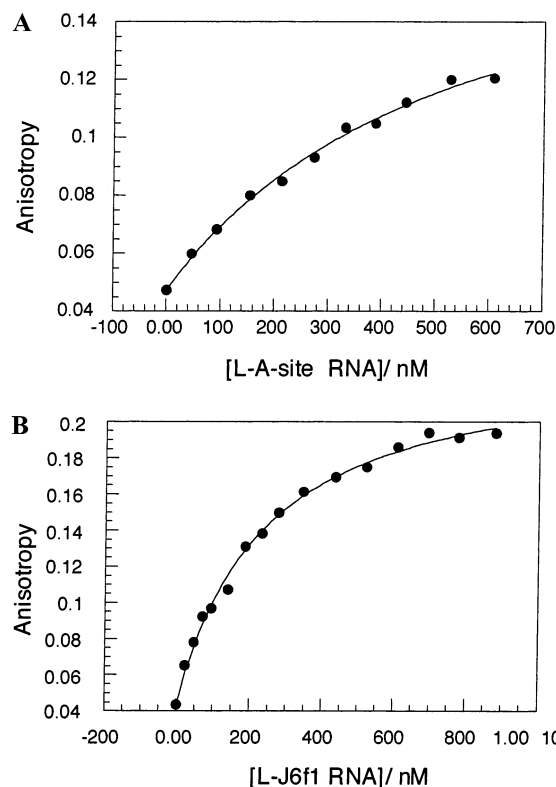
^a CRP. ^b CRT. ^c Not determined.

FIGURE 2: (A, B) Fluorescence anisotropy of fluorescently labeled paromomycin (CRP) (20 nM) as a function of L-RNA construct A-site (A) concentrations and fluorescence anisotropy of fluorescently labeled tobramycin (CRT) (20 nM) as a function of L-RNA construct J6f1 (B) concentration. In these experiments, increasing concentrations of the RNA constructs were added to CRP or CRT under the conditions described in Materials and Methods.

molar range are to be expected in the naturally occurring series. Control experiments with commercially prepared Dharmacon A-site RNA constructs produced the same results as the experiments with A-site construct, synthesized in our laboratory.

Binding of D- and L-Neamine to D- and L-A-Site RNA Constructs. Given the stereochemical results described above, the enantiomeric aminoglycoside L-neamine (Scheme 2) was synthesized and tested as a competitive inhibitor for CRP binding to the A-site constructs described above (Table 1). The binding of L-neamine to both the D- and L-A-site constructs was compared to the binding of the naturally occurring enantiomer D-neamine. Straightforward competitive binding of L-neamine to the RNA constructs was observed. D-Neamine binds with an approximately 2-fold higher affinity to the D-construct than does L-neamine (Table 1). Conversely, L-neamine binds with a 2-fold higher affinity than D-neamine does to the L-A-site RNA. Naturally occurring neomycin B

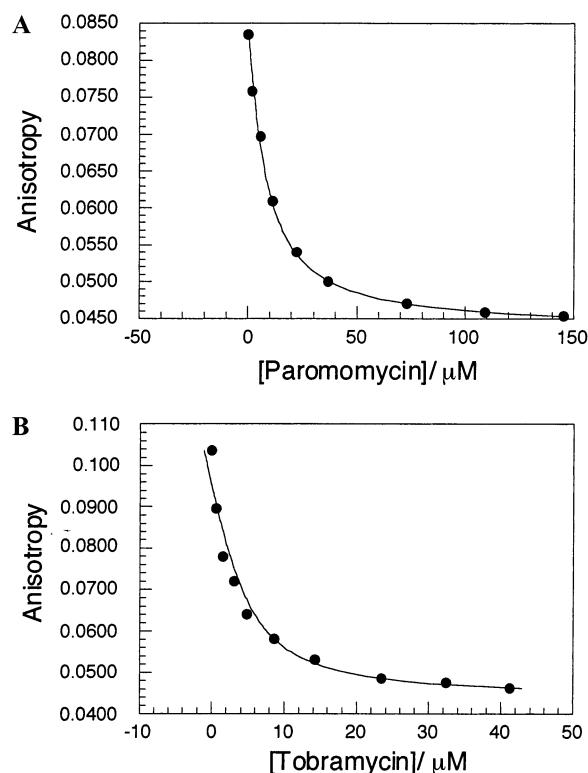


FIGURE 3: (A, B) Fluorescence anisotropy of fluorescently labeled paromomycin (CRP) (20 nM) containing L-RNA construct A-site (A) as a function of paromomycin concentrations and fluorescence anisotropy of fluorescently labeled tobramycin (CRT) (20 nM) containing L-RNA construct J6f1 (B) as a function of tobramycin concentrations.

binds to the D-A-site RNA construct with an approximately 2-fold higher affinity than to the L-RNA construct (Table 1). Overall, these results indicate a very modest degree of stereospecificity in aminoglycoside-decoding region rRNA binding.

Aminoglycoside Binding to Ribosomes. The experiments reported above demonstrate that the binding of D/L-neamine to prokaryotic decoding region constructs is only weakly stereospecific. These studies are extended to measurements on intact ribosomes. Initial experiments were focused on the extension of the described fluorescence anisotropy method to accurately measure aminoglycoside binding to intact ribosomes. Measurements of this type had previously been attempted by equilibrium dialysis using radioactive aminoglycosides (29). This method is somewhat cumbersome and time-consuming, and requires the use of radioactive tracers. In the studies reported here, the fluorescence anisotropy methodology already described (15–18, 21) for the measurement of aminoglycoside binding to RNA constructs is adapted for use with intact ribosomes.

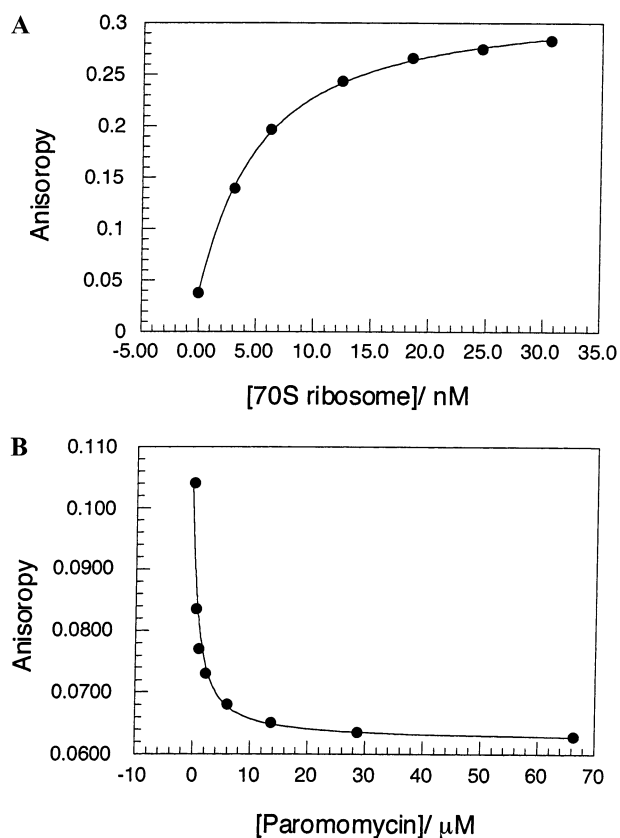


FIGURE 4: (A, B) Fluorescence anisotropy of fluorescently labeled paromomycin (CRP) (20 nM) as a function of 70S (A) ribosomes concentrations. In these experiments, increasing concentrations of the ribosomes were added to CRP under the same conditions described in Materials and Methods. Fluorescence anisotropy of fluorescently labeled paromomycin (CRP) (20 nM) containing 70S ribosomes, as a function of paromomycin (B) concentrations.

In the experiments reported here, CRP (Scheme 2) is used as the fluorescent probe to monitor binding (21). Figure 4A provides data demonstrating the high affinity and saturable binding of CRP to *E. coli* 70S ribosomes. Competition experiments with several aminoglycosides provided binding data consistent with expectations based on previous equilibrium dialysis measurements (29). Figure 4B shows a representative example of competition binding data for 70S ribosomes with paromomycin (Scheme 1). As expected, streptomycin did not effectively compete with CRP for binding to bacterial ribosomes. Thus, the K_D value was not determined for streptomycin in the CRP-competition assay. Streptomycin is not thought to compete with the aminoglycosides for binding to sites on ribosomes (29, 30). The dissociation constants for various aminoglycosides bound to 70S ribosomes are summarized in Table 2. These data are in reasonable accord with published measurements made using a radio ligand binding assay (29). For example, tobramycin and kanamycin were reported to bind with K_D s = 1.4 and 1.7 μ M, respectively (29).

Similar experiments were performed with yeast 80S ribosomes. It was established that aminoglycoside antibiotics bind to *E. coli* and yeast ribosomes with comparable affinities (Table 2). Interestingly, streptomycin was found to compete with CRP for 80S ribosome binding, producing a K_D value of 30.5 μ M, indicating differences in the mode of streptomycin interaction with 80S and 70S ribosomes.

Table 2: Dissociation Constants of Aminoglycoside Complexes with 70S and 80S Ribosomes (K_d , K_D , μ M)

aminoglycoside	70S ribosome	80S ribosome
CRP (K_d)	0.0037 ± 0.0011	0.0032 ± 0.0009
neomycin B	0.14 ± 0.038	0.11 ± 0.014
paromomycin	1.41 ± 0.15	1.97 ± 0.10
kanamycin B	1.51 ± 0.46	2.63 ± 0.52
tobramycin	1.76 ± 0.38	3.69 ± 0.31
streptomycin	NB ^a	30.5 ± 2.33
D-neamine	5.45 ± 0.68	1.14 ± 0.25
L-neamine	2.69 ± 0.46	6.06 ± 0.63

^a Negligible binding. Only a slight (<10%) decrease in fluorescence anisotropy of CRP-70S ribosome complex was observed with streptomycin concentrations of up to 10 mM. Higher concentrations of streptomycin were not tested.

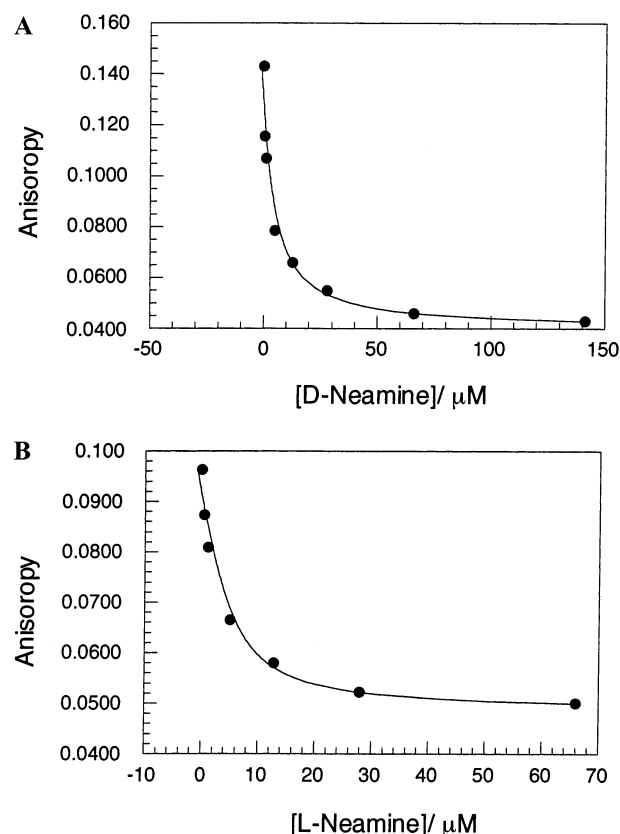


FIGURE 5: (A, B) Fluorescence anisotropy of fluorescently labeled paromomycin (CRP) (20 nM) containing 70S ribosomes as a function of D-neamine (A) and L-neamine (B) concentrations.

Binding of D- and L-Neamine to Bacterial and Yeast Ribosomes. On the basis of the results reported above, the fluorescence binding assay method was used to determine the stereospecificity of the binding of aminoglycosides to ribosomes. These experiments were carried out with naturally occurring D-neamine (22, 27) and its synthetic enantiomer L-neamine (Scheme 1). The competitive binding isotherms for the binding of D and L-neamine are shown in Figure 5A,B, and the binding data for the isomers are summarized in Table 2. Most importantly, both L- and D-neamine bind to *E. coli* and yeast ribosomes with comparable affinities. In fact, L-neamine binds to the bacterial ribosomes with an approximately 2-fold higher affinity than does the natural D-neamine. However D-neamine was found to be a 5-fold better binder for yeast ribosome than L-neamine. These experiments establish that stereospecificity of aminoglycoside

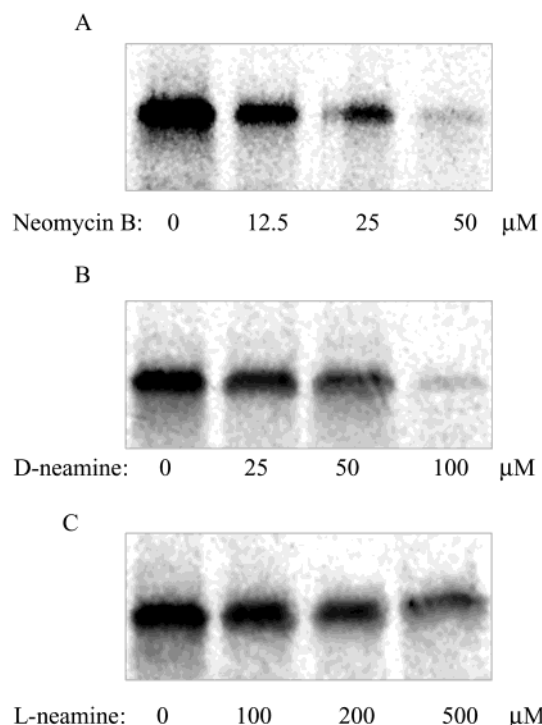


FIGURE 6: (A–C) In vitro translation in the presence of aminoglycosides: (A) neomycin B, (B) D-neamine, (C) and L-neamine.

binding to intact ribosomes is low, and in this sense, the results obtained with the A-site rRNA constructs are predictive.

Inhibition of Translation by D- and L-Neamine. The binding results described above provide no information on the functional consequences of the binding of D/L-neamines to ribosomes. To approach this issue, we determined the effects of these aminoglycosides on protein translation. D- and L-neamine were analyzed with regard to their potencies as inhibitors of in vitro translation. Neomycin B was used as a control aminoglycoside. Figure 6 shows the results of typical in vitro translation reactions in the presence of neomycin B (A), D-neamine (B), and L-neamine (C). As expected, the aminoglycosides were found to effectively inhibit in vitro translation. IC₅₀, 50% inhibitory concentration, was defined as the concentrations of aminoglycoside producing 50% inhibition of translation. Quantitation of the gel bands provided the following IC₅₀ values: neomycin B, 15 μM; D-neamine, 38 μM; and L-neamine, 195 μM. These functional assays indicate a clear stereoselective advantage of D-neamine versus its unnatural L-neamine enantiomer.

Antibiotic Activity Disk Assays. The functional data described above predict that D-neamine will be a more potent antibacterial agent than its L-enantiomer. Two Gram(–) bacterial strains (*E. coli* (ATCC 25922) and *P. aeruginosa* (ATCC 27853)) were investigated. These two strains were chosen for two reasons. First, they are both Gram(–), and aminoglycosides preferentially inhibit the growth of Gram(–) bacteria (1, 2, 6). Second, both species can become resistant to aminoglycosides by mechanisms involving the enzymatic modification of these drugs (6). A potentially attractive property of mirror-image aminoglycosides is that they might avoid resistance mechanisms that depend on stereospecific interactions between modifying enzymes and their aminoglycoside substrates.

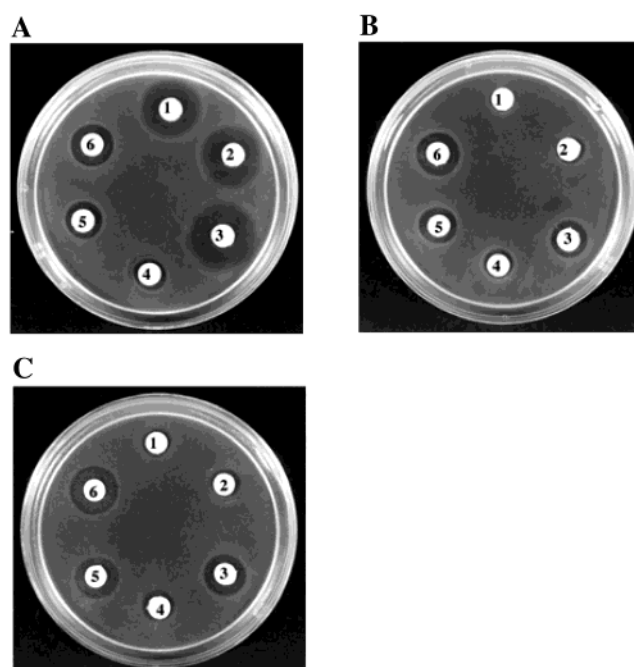


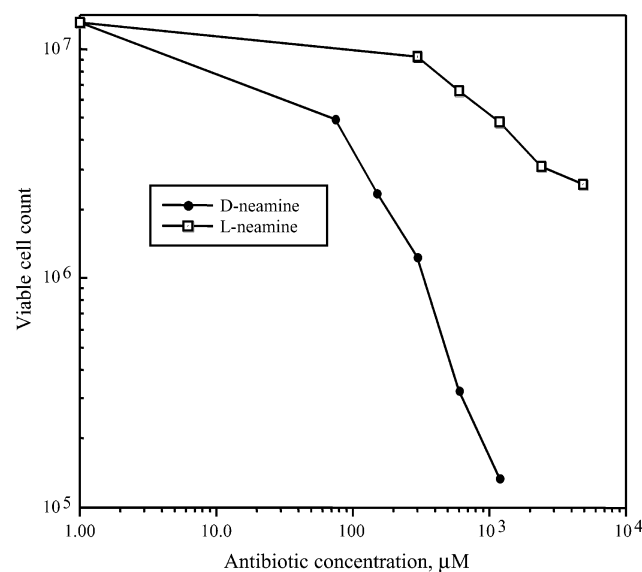
FIGURE 7: (A–C) Antibiotic activity disk assay of *E. coli* (ATCC 25922) wild type (A) and transformed with the plasmid pMM, bearing the APH(3')IIa gene (B), *P. aeruginosa* (ATCC 27853) (C). 1, D-neamine (100 nmol); 2, D-neamine (200 nmol); 3, D-neamine (500 nmol); 4, L-neamine (200 nmol); 5, L-neamine (500 nmol); 6, L-neamine (1000 nmol).

Antibiotic disk assays were used for the estimation of antibacterial activities of L-neamine and D-neamine. As expected, L-neamine proved to possess antibacterial activity. L-Neamine displayed a somewhat lower activity with WT *E. coli* (ATCC 25922) than D-neamine (Figure 7A) but was still clearly active. Interestingly, when *E. coli* kanamycin/neomycin-resistant bacteria were studied, the activity of D-neamine was essentially abolished, while L-neamine showed almost the same activity as that observed with nonresistant WT *E. coli* (Figure 7B). Aminoglycoside resistance of *E. coli* was then induced by transformation of the bacteria with a pMM plasmid which contains the gene for aminoglycoside phosphotransferase APH(3') IIa, also called neomycin phosphotransferase (NTP II) (26). This gene is derived from the Tn5 transposon and comprises a generic antibiotic marker for kanamycin and neomycin resistance (26). In a second set of experiments, the sensitivity of *P. aeruginosa* (ATCC 27853) toward the enantiomeric neamines was studied. Both D-neamine and L-neamine showed similar activities in this case (Figure 7C). *P. aeruginosa* is naturally resistant to aminoglycosides due to the presence of the APH(3') IIB phosphotransferase gene in its genome. The APH(3') IIB of *P. aeruginosa* is homologous to the above-mentioned APH(3') IIa of *E. coli* (26). The decreased activity of D-neamine observed here is doubtless related to its partial selective deactivation, while the activity of L-neamine remains essentially unchanged (with respect to WT *E. coli*).

Minimal Inhibitory Concentrations of the Neamines. Minimal inhibitory concentrations (MIC) of D- and L-neamine were measured in WT *E. coli*, kanamycin/neomycin-resistant *E. coli*, and in *P. aeruginosa*. The results are summarized in Table 3. The bactericidal profiles for D- and L-neamine are also presented in Figure 8. As can be seen here, both compounds are bactericidal toward *E. coli* (ATCC 25922).

Table 3: Minimal Inhibitory Concentrations (MIC) of D- and L-Neamine (μM)

drug	<i>E. coli</i>	<i>E. coli</i> kan/neo resistant	<i>P. aeruginosa</i>
D-neamine	150	>6400	500
L-neamine	1300	2100	1600

FIGURE 8: Bactericidal profiles of D- and L-neamine against *E. coli* (ATCC 25922) after 3 h incubation with antibiotics. Each point is the average of duplicate measurements.

However the activity of L-neamine is significantly lower than that for natural D-neamine under the conditions of the experiments. D-Neamine begins to kill bacteria at $75 \mu\text{M}$, while the bactericidal effects of L-neamine manifest at $600 \mu\text{M}$ and, thus, the latter aminoglycoside is approximately 8 times less potent than its enantiomer. This ratio is confirmed by MIC measurements as L-neamine is observed to be approximately 8.7 times less active than D-neamine. However, it is important to note that while the MIC values for L-neamine are close for the resistant and susceptible bacterial strains, there is a sharp drop off for D-neamine in the resistant strains. This is especially true for the resistant *E. coli* strain (Table 3).

DISCUSSION

The experiments described here were designed to further probe the specificity of aminoglycoside–target interactions. It is generally accepted that aminoglycosides can bind to a myriad of RNA structures that contain nonduplex regions (15). An important question to address is how specifically aminoglycosides bind to their pharmacological target, namely, the A-site rRNA decoding region of susceptible bacteria (3, 5, 19, 20, 31, 32). Published binding experiments on prokaryotic A-site decoding region RNA constructs measured affinities in the $1\text{--}2 \mu\text{M}$ range, save for neomycin B, which exhibits a somewhat higher affinity (18, 21). The fact that the measured affinities of the structurally diverse aminoglycosides are similar suggests that binding is class specific, rather than being specific with respect to a particular molecule. This is also true in vivo, since structurally diverse aminoglycosides are effective antibiotics (6). This is not to say that there is little to no specificity in binding, since NMR

investigations on the binding of aminoglycosides to the truncated A-site decoding region construct B suggest elements of specificity in the binding (19, 20). In addition, the recent extraordinary structural studies on ribosomal subunits also demonstrate specificity in A-site interactions with mRNA and tRNA codon–anticodon complexes as well as with aminoglycosides (31–34). Some of these data indicate how the aminoglycoside paromomycin distorts decoding region interactions facilitating the binding of near cognate tRNAs (33).

The fact that structural studies may identify specific interactions between aminoglycosides and decoding region RNA can be readily reconciled with the limited structural specificity mentioned above found in the binding aminoglycosides to decoding region construct and ribosome. It is reasonable to suggest that the inherent flexibility of RNA and the aminoglycosides may allow for a myriad of different binding solutions, which lead to the same functional consequences. To further examine the limits of binding specificity to a bacterial A-site decoding region construct, we determined the stereospecificity of aminoglycoside binding to the mirror image decoding region construct.

In the initial binding experiments reported here, aminoglycoside binding to the mirror-image prokaryotic rRNA A-site constructs was measured. In all cases except for kanamycin, the naturally occurring aminoglycosides showed a modest 2–3-fold selectivity for the D-series RNA construct. In the case of kanamycin, binding to the unnatural L-RNA was favored by a factor of approximately 1.5 over the D-decoding region construct. The general drift toward enhanced binding of the cognate RNA construct was also observed in the case of D and L-neamine. Both enantiomers were preferentially bound to their stereochemical cognate by a factor of approximately 2-fold relative to the enantiomers.

An important question to address is whether the weak stereospecific binding observed with the decoding region constructs is inherent in general in the interactions of conformationally flexible aminoglycosides with flexible RNA constructs, or is the weak stereospecificity simply a function of decoding region construct binding? The decoding region construct described here binds aminoglycosides in the μM range, an affinity typical of many aminoglycoside RNA interactions (7–14). It was of interest to determine whether significant stereospecificity is observed in instances where the binding affinities and specificities are considerably enhanced. The truncated RNA aptamer (J6f1) binds tobramycin with a $K_D = 5 \text{ nM}$ and distinguishes in binding among structurally similar aminoglycosides (Table 2), although not as strongly as the full-length constructs (16). The enantiomer of J6f1 binds tobramycin with a $K_D = 2.2 \mu\text{M}$ (Table 2) and has thus reverted to the binding affinity typical of many quasispecific aminoglycoside–RNA binding events, including aminoglycoside binding by the decoding region constructs. Not only has the binding affinity of enantiomeric J6f1 for tobramycin decreased by 420-fold, but the specificity of binding for tobramycin is substantially decreased (Table 2). These experiments demonstrate that strong stereospecificity of aminoglycoside binding does occur in the case of specific tight binding RNA aptamers and is not simply a function of innate ligand–receptor flexibility.

Footprinting studies were undertaken in order to determine whether differences in the binding of the stereoisomers might

be observable (see Supporting Information). It was of interest to determine whether the stereoisomers bound to the RNA molecules in the same or similar ways. D- and L-neamine were found to bind to the same site on the D-RNA construct as well as the same site on the L-RNA construct. However, the binding site on the L-RNA construct is distinct from the binding site on the D-RNA construct. The aminoglycoside binding site on the D-RNA construct is defined by the pocket produced by the nucleotides: C6–G22, A7•A21, and A20 (see Supporting Information). This is in good accordance with previous results (19, 20). Interestingly, the binding site on the L-RNA decoding region construct is formed by the nucleotides: A7•A21, A9, C10–G17. In other words, the D-RNA aminoglycoside binding site is located “below” the A-rich bulge, and the L-RNA aminoglycoside binding site is located “above” the A-rich bulge. Neomycin B binds similarly to D- and L-neamine but spans a more extensive portion of the RNA than do the simpler aminoglycosides (Supporting Information).

The results described above demonstrate a marginal stereospecificity (2–3-fold) in the binding of aminoglycosides to A-site decoding region rRNA constructs. These studies were then expanded to a more biological realm to include studies on ribosomes and bacteria. In initial studies, aminoglycoside binding to *E. coli* ribosomes was measured using fluorescence anisotropy methods previously developed in this laboratory (15–18, 21). CRP (Scheme 1) was used as the binding probe (21). As reported here, the fluorescence assay was found to be apparently well adapted to measuring aminoglycoside binding to 70S bacterial ribosomes (*E. coli*). Save for neomycin B, where the dissociation constant is approximately 0.1 μM , the dissociation constants measured for other aminoglycosides were in the 1–2 μM range. These data are quite consistent with measurements made on the A-site decoding region constructs (18, 21) and data from direct measurements on radioactive aminoglycoside binding to intact *E. coli* ribosomes (29). In addition, streptomycin, which is not thought to bind with high affinity to the A-site decoding region in bacteria (29, 30, 32), did not exhibit measurable binding in the assay. The fact that the measured binding constants for aminoglycosides to the ribosomes and A-site construct are so close is not surprising inasmuch as structural studies on the 30S ribosomal subunit show that the A-site decoding region is not in close association with proteins in the ribosome (31–34). Furthermore, X-ray structural studies on the 30S subunit also show that the A-site decoding region is probably similar in structure to the 27 nt decoding region construct whose structure was determined by NMR spectroscopy (19, 20, 31, 32).

The stereospecificity of aminoglycoside binding to *E. coli* ribosomes was then determined using the fluorescence method described above using D- and L-neamine as the competing aminoglycosides. As expected from model studies on the A-site construct, both L- and D-neamine both bound to the ribosomes. In fact, L-neamine bound to *E. coli* ribosomes with a 2-fold greater affinity than did D-neamine. Small and large subunits were not tested independently because while the A-site decoding region resides on the small 30S subunit, there is also some measured aminoglycoside binding associated with the larger 50S subunit (29).

Experiments with yeast 80S ribosomes showed great similarity in the affinities of aminoglycosides to prokaryotic

(*E. coli* 70S) and eukaryotic (*S. cerevisiae* 80S) ribosomes. Interestingly, it was possible to assign a K_D of 30.5 μM for streptomycin binding to the 80S ribosome, while no competition with CRP for 70S ribosome binding was observed. This might be an indication that streptomycin, and possibly all aminoglycosides, bind to eukaryotic and prokaryotic ribosomes in a different manner. In addition, D-neamine appeared to be a 5-fold stronger yeast ribosome binder than L-neamine, which is opposite to the results obtained with *E. coli* ribosomes. This indicates differences in the mode of eukaryotic and prokaryotic ribosomal recognition of these compounds.

The binding experiments described above offer no insights into the functional consequences of aminoglycoside binding to the ribosomes. To approach this issue, we studied the functional consequences of D- and L-neamine binding on in vitro translation reactions. Protein translation was performed using chloramphenicol acetyl transferase (CAT) mRNA. CAT mRNA was transcribed from a plasmid, bearing the CAT gene under the control of the T7 promoter (35, 36). A commercial *E. coli* ribosomal suspension was supplemented with an *E. coli* extract containing the required elements for translation. These include translation factors, tRNAs, and aminoacyl tRNA synthetases. Plasmid, T7 RNA polymerase, and amino acids were added to the reaction mixture, and both transcription and translation steps were performed in the same vial (35, 36). The effects of the aminoglycosides on the translation process were evaluated by measuring the incorporation of ^{35}S methionine in the translated chloramphenicol acetyl transferase protein. Both D- and L-neamine are capable of inhibiting protein synthesis in vitro. However, D-neamine appeared to be over 5-fold more potent as a translation inhibitor than L-neamine. This result shows that the ribosomal binding data per se is not quantitatively predictive with respect to the functional potencies of aminoglycosides. The 70S ribosomal binding studies actually showed a small 2-fold difference in binding affinity between D- and L-neamines, with the L-neamine binding with greater affinity. In the functional assay D-neamine proved to be approximately 5-fold more potent than its enantiomer. There are at least two possible reasons for this observed disparity. First, it is possible that the measurements of ribosome–aminoglycoside binding provide average dissociation constants for several different binding sites with similar dissociation constants. Only binding at the A-site is crucial for the inhibition of translation. The notion of multiple aminoglycoside binding sites runs counter to previous chemical protection experiments performed on ribosomes, not to mention NMR and X-ray structural studies, which suggest a localized binding site for aminoglycosides at the decoding region (19, 20, 31, 32). However, binding measurements and chemical protection experiments measure entirely different phenomena. In fact, given the broad range of RNA structures that aminoglycosides bind to, it would be surprising if a structure as complicated as a ribosome only possessed a single aminoglycoside binding site (19, 20). A second reason for the disparity in measurements is that it is entirely possible that the structure of the decoding region is altered during translation. This could have the effect of altering binding affinities for aminoglycosides, so that binding measurements made on quiescent ribosomes are not quantitatively relevant to aminoglycoside binding to ribosomes during translation,

with all of the various factors and mRNA interacting with the ribosome.

To extend the experiments described above, D- and L-neamines were tested as bactericidal drugs of the Gram-(−) strain WT *E. coli* (ATCC 25922). In these assays, the abilities of the antibiotics to kill the bacteria is measured as the log of the number of viable bacteria following a short-term treatment with the antibiotics (28). Aminoglycosides are generally known to be bactericidal (1, 2, 6). Importantly, both D- and L-neamine are bactericidal, and therefore, the binding of L-neamine to ribosomes has the same functional consequence as the binding of D-neamine. Both D- and L-neamine exhibit very weak activity against Gram-(+) bacteria, a hallmark of aminoglycoside action (6). For example, when tested against *Streptomyces aureus* and *Enterococcus faecalis*, L-neamine proved not to have anti-bacterial activity (unpublished experiments). In the case of *E. coli*, the natural D-neamine proved to be 8- to 9-fold more potent than its L-enantiomer. This modest stereospecificity observed is in line with results from the translation assay described above. The relative minor difference of 5-fold selectivity measured in the translation assay to 8–9-fold measured in the antibacterial assay might be related to cellular uptake. While the actual mechanism of membrane permeability to cationic aminoglycosides has not been clarified on a molecular level, it is likely that the process involves membrane channels and protein transporters (37–41). It is then possible that the transmembrane transport of aminoglycosides behaves modestly stereoselectively and that L-neamine is transported with lowered efficiency compared to its D-enantiomer. In addition to measuring the antibacterial activity of the neamines against susceptible WT *E. coli*, they were also tested against aminoglycoside-resistant bacteria.

Interestingly, when the WT *E. coli* strain was transformed with plasmid pMM bearing the gene for the aminoglycoside kinase APH(3')IIa which confers kanamycin resistance, selective interference with the antibiotic activity of D-neamine was observed. Activity of D-neamine against this resistant *E. coli* strain decreased by a factor of over 40, compared to that of WT *E. coli*. In contrast, the activity of L-neamine toward resistant *E. coli* did not significantly change. Moreover, when the enantiomers of neamine were tested against the naturally aminoglycoside-resistant *P. aeruginosa* strain, activities of both D- and L-neamines proved to be similar, suggesting enhanced resistance of this strain to D-neamine. Insofar as aminoglycoside metabolizing enzymes, such as APH(3')IIa, are themselves stereospecific for aminoglycoside substrates, enantiomeric aminoglycosides might escape relevant resistance mechanisms but still be effective in binding to their target bacterial rRNA molecules. Some of the enzymes described which render aminoglycosides inactive include the acetylases, the adenylases, and the kinases (1, 2, 5, 6). Since bacterial resistance to the aminoglycosides most frequently occurs through extrinsic, metabolic means, and not through mutations in the target rRNAs (1, 2, 5, 6), aminoglycoside analogues which escape these modification reactions could be of substantial use. This possibility will need to be further explored with other resistant bacteria and more potent enantiomeric aminoglycosides.

In conclusion, modest stereospecificity of aminoglycoside effects are found in the functional activities of D- and

L-neamines. The use of mirror-image aminoglycosides may be advantageous in the treatment of resistant bacterial infections inasmuch as the L-series aminoglycosides may not be processed by stereospecific aminoglycoside processing enzymes. It is also possible that L-aminoglycosides might be less toxic than their D-counterparts.

SUPPORTING INFORMATION AVAILABLE

Footprinting studies on the binding sites of the D- and L-neamines on the D- and L-A-site RNA constructs. This material is available free of charge via the Internet at <http://pubs.acs.org>.

REFERENCES

- Gale, E. F., Cundliffe, E., Reynolds, P. E., Richmond, M. H., and Waring M. J. (1981) *The Molecular Basis of Antibiotic Action*, 2nd ed., pp 419–439, John Wiley & Sons, London.
- Cundliffe, E. (1989) *Annu. Rev. Microbiol.* 43, 207–233.
- Noller, H. F. (1991) *Annu. Rev. Biochem.* 60, 191–227.
- Woodcock, J., Moazed, D., Cannon, M., Davies, J., and Noller, H. F. (1991) *EMBO J.* 10, 3099–3103.
- Cundliffe, E. (1990) *The Ribosome: Structure, Function & Evolution* (Hill, W. E., Dahlberg, A. E., Garret, R. A., Moore, P. B., Schlessinger, D., and Warner, J. R., Eds.), pp 479–490, American Society for Microbiology, Washington, DC.
- Chambers, H. F., and Sande, M. A. (1996) Goodman & Gilman's *The Pharmacological Basis of Therapeutics* (Hardman, J. G., Limbird, L. E., Molinoff, P. B., Ruddon, R. W., and Gilman, A. G., Eds.) 9th ed., Chapter 46, pp 1103–1121, McGraw-Hill, New York.
- Zapp, M. L., Stern, S., and Green, M. R. (1993) *Cell* 74, 969–978.
- Werstuck, G., Zapp, M. L., and Green, M. R. (1996) *Chem. Biol.* 3, 129–137.
- Mei, H. Y., Cui, M., Heldsinger, A., Lemrow, S. M., Loo, J. A., Sannes-Lowery, K. A., Sharmeen, L., and Czarnik, A. W. (1998) *Biochemistry* 37, 14204–14212.
- Tok, J. B., Cho, J., and Robert, R. R. (1999) *Biochemistry* 38, 199–206.
- Stage, T. K., Hertel, K. J., and Uhlenbeck, O. C. (1995) *RNA* 1, 95–101.
- Wang, Y., and Rando, R. R. (1995) *Chem. Biol.* 2, 281–290.
- Lato, S. M., Boles, A. R., and Ellington, A. D. (1995) *Chem. Biol.* 2, 291–303.
- Wallis, M. G., Von Ahsen, U., Schroeder, R., and Famulok, M. (1995) *Chem. Biol.* 2, 543–552.
- Cho, J., Hamasaki, K., and Rando, R. R. (1998) *Biochemistry* 37, 4985–4992.
- Hamasaki, K., Killian, J. Cho, J., and Rando, R. R. (1998) *Biochemistry* 37, 656–663.
- Cho, J., and Rando, R. R. (1999) *Biochemistry* 38, 8548–8554.
- Ryu, D. H., and Rando, R. R. (2001) *Bioorg. Med. Chem.* 9, 2601–2608.
- Fourmy, D., Recht, M. I., Blanchard, S. C., and Puglisi, J. D. (1996) *Science* 274, 1367–1371.
- Lynch, S. R., and Puglisi, J. D. (2001) *J. Mol. Biol.* 306, 1037–1058.
- Wang, Y., Hamasaki, K., and Rando, R. R. (1997) *Biochemistry* 36, 768–779.
- Roestamadj, J., Grapsas, I., and Mobashery, S. (1995) *J. Am. Chem. Soc.* 117, 11060–11069.
- Wincott, F., DiRenzo, A., Shaffer, C., Grimm, S., Tracz, D., Workman, C., Sweedler, D., Gonzalez, C., Scaringe, S., and Usman, N. (1995) *Nucl. Acid Res.* 23, 2677–2684.
- Rheinberger, H.-J. Geigenmuller, U., Wedde, M., and Nierhaus, K. H. (1988) *Methods Enzymol.* 164, 658–662.
- Verschuur, A., Warner, J. R., Srivastava, S., Grassucci, R. A., and Frank, J. (1997) *Nucl. Acid Res.* 26, 655–661.
- Wright, G. D., and Thompson, P. R. (1999) *Front. Biosci.* 4, D9–21.
- Greenberg, W. A., Priestley, E. S., Sears, P. S., Alper, P. B., Rosenbohm, C., Hendrix, M., Hung, S.-C., and Wong, C.-H. (1999) *J. Am. Chem. Soc.* 121, 6527–6541.

28. Morrissey, I., and George, J. T. (2000) *J. Antimicrob. Chemother.* 45, 107–110.
29. Le Goffic, F., Capmau, M.-L., Tangy, F., and Baillarge, M. (1979) *Eur. J. Biochem.* 102, 73–81.
30. Spickler, C., Brunelle, M.-N., and Brakier-Gingras, L. (1997) *J. Mol. Biol.* 273, 586–599.
31. Wimberly, B. T., Brodersen, D. E., Clemons, W. M., Jr., Morgan-Warren, R. J., Carter, A. P., Vonrhein, C., Hartsch, T., and Ramakrishnan, V. (2000) *Nature* 407, 327–339.
32. Carter, A. P., Clemons, W. M., Brodersen, D. E., Morgan-Warren, R. J., Wimberly, B. T., and Ramakrishnan, V. (2000) *Nature* 407, 340–348.
33. Ogle, J. M., Brodersen, D. E., Clemons, W. M., Jr., Tarry, M. J., Carter, A. P., and Ramakrishnan, V. (2001) *Science* 292, 897–902.
34. Yusupov, M. M., Yusupova, G. Z., Baucom, A., Lieberman, K., Earnest, T. N., Cate, J. H. D., and Noller, H. F. (2001) *Science* 292, 883–896.
35. Ambion (2000) PROTEINscript-PRO Linked Transcription:Translation Kit. *Ambion Instruction Manual*, Austin, TX.
36. Pratt J. M. (1984) Coupled Transcription-Translation in Prokaryotic Cell-Free System, in *Transcription and Translation* (Hames, B. C., and Higgins, S. J.), pp 179–209, IRL Press, Oxford.
37. Leviton, I. M., Fraimow, H. S., Carrasco, N., Dougherty, T. J., and Miller, M. H. (1995) *Antimicrob. Agents Chemother.* 39, 467–475.
38. Taber, H. W., Mueller, J. P., Miller, P. F., and Arrow, A. S. (1987) *Microbiol. Rev.* 51, 439–457.
39. Mates, S. M., Eisenberg, E. S., Mandel, L. J., Patel, L., Kaback, H. R., and Miller, M. H. (1982) *Proc. Natl. Acad. Sci. U.S.A.* 79, 6693–6697.
40. Chopra, I. (1988) *Parasitology* 96, S25–S44.
41. Davis, B. D., Chen, L. L., and Tai, P. C. (1986) *Proc. Natl. Acad. Sci. U.S.A.* 83, 6164–6168.

BI026086L